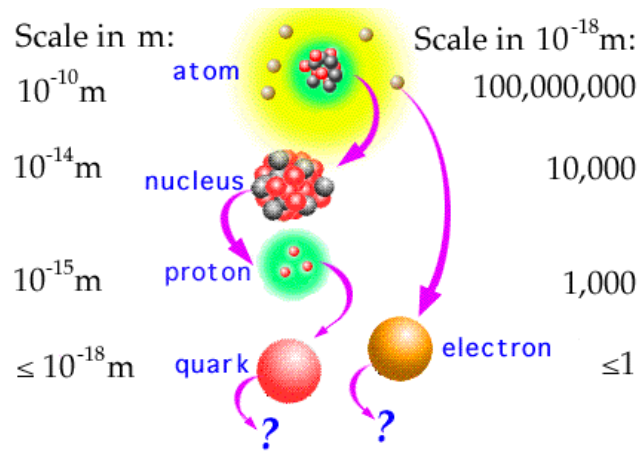


Electric, Magnetic and Axial Form Factors from Lattice QCD

Rajan Gupta

Theoretical Division

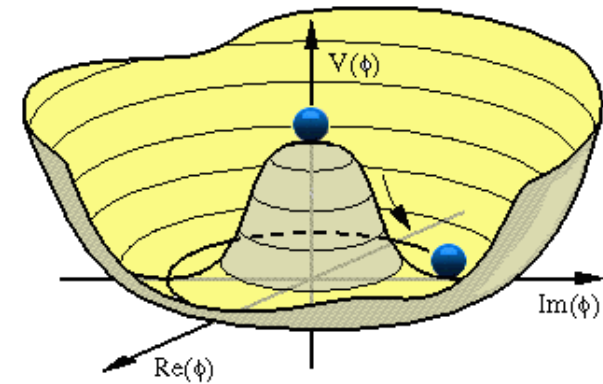
Los Alamos National Laboratory, USA



Elementary Particles

	Quarks	Leptons	
I	u up	ν_e electron neutrino	e electron
II	c charm	ν_μ muon neutrino	μ muon
III	t top	ν_τ tau neutrino	τ tau
	Force Carriers		
	γ photon	Z Z boson	W W boson
	g gluon		

Three Families of Matter



PNDME Collab.

clover-on-HISQ

- Tanmoy Bhattacharya
- Vincenzo Cirigliano
- Yong-Chull Jang
- Huey-Wen Lin
- Sungwoo Park
- Boram Yoon

Gupta et al, PRD96 (2017) 114503

Gupta et al, PRD98 (2018) 034503

Lin et al, PRD98 (2018) 094512

Gupta et al, PRD98 (2018) 091501

NME Collab.

clover-on-clover

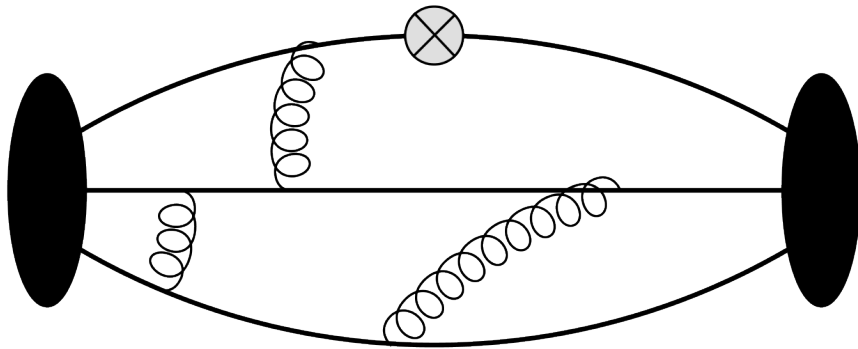
- Tanmoy Bhattacharya
- Vincenzo Cirigliano
- Yong-Chull Jang
- Balint Joo
- Huey-Wen Lin
- Kostas Orginos
- Sungwoo Park
- David Richards
- Frank Winters
- Boram Yoon

Outline

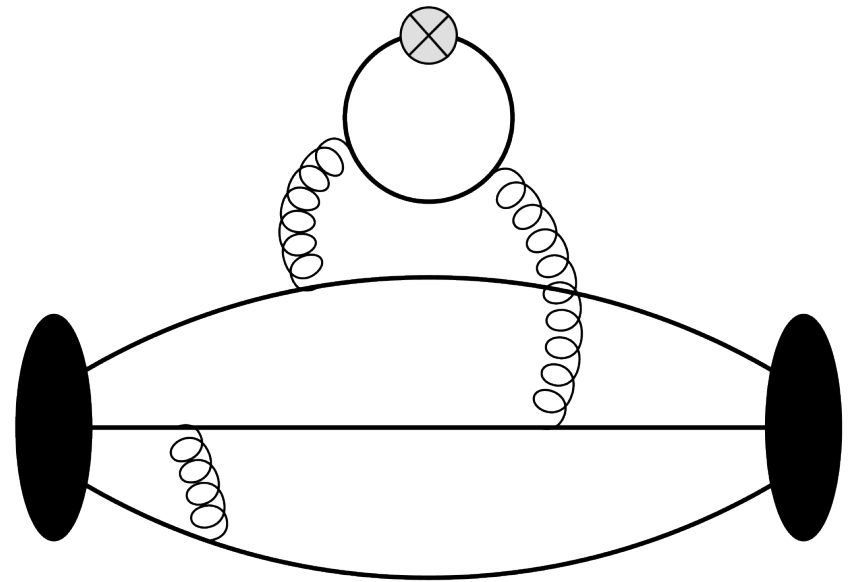
- Physics Motivation
 - Electric and Magnetic form factors extracted from electron and muon scattering
 - Axial vector form factors of nucleon needed for the analysis of neutrino-nucleus scattering:
 - Monitoring neutrino flux
 - Cross-section off various nuclear targets (LAr)
- Challenge: controlling systematic errors in the lattice QCD calculations of the matrix elements of axial and vector current operators within nucleon states

See Community White Paper: [arXiv:1904.09931](https://arxiv.org/abs/1904.09931)

High precision estimates of the matrix elements of quark bilinear operators within the nucleon state, obtained from “connected” and “disconnected” 3-point correlation functions, are needed to address a number of important physics questions



Connected



Disconnected

Matrix elements within nucleon states required by many experiments

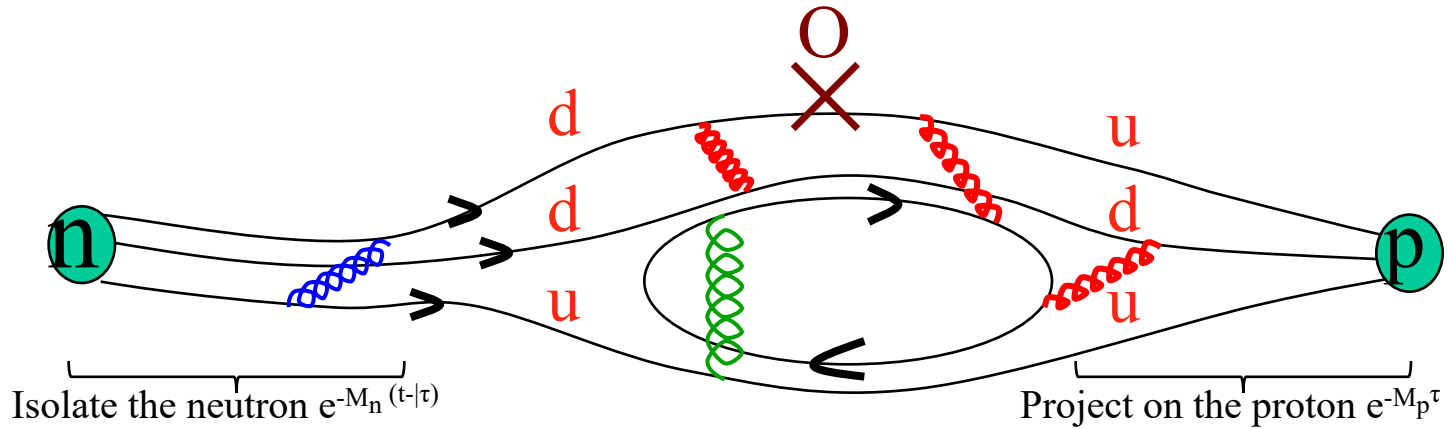
- Isovector charges g_A, g_S, g_T $\langle p | \bar{u} \Gamma d | n \rangle$
- Axial vector form factors $\langle p(q) | \bar{u} \gamma_\mu \gamma_5 d(q) | n(0) \rangle$
- Vector form factors $\langle p(q) | \bar{u} \gamma_\mu d(q) | n(0) \rangle$
- Flavor diagonal matrix elements $\langle p | \bar{q} q | p \rangle$
- nEDM: Θ -term, quark EDM, quark chromo EDM, Weinberg operator, 4-quark operators
- $0\nu\beta\beta$
- Generalized Parton Distribution Functions

e, μ, ν - Z scattering 5 Form Factors

- $G_E(Q^2)$ Electric
- $G_M(Q^2)$ Magnetic
- $G_A(Q^2)$ Axial
- $\tilde{G}_P(Q^2)$ Induced pseudoscalar
- $G_P(Q^2)$ Pseudoscalar
- The lattice methodology is the same
- Precise experimental data exist for $G_E(Q^2)$ and $G_M(Q^2)$
- Axial ward identity relates $G_A(Q^2)$, $\tilde{G}_P(Q^2)$, $G_P(Q^2)$

Lattice QCD has to predict all 5, g_A , μ

Calculating matrix elements using Lattice QCD



$$\begin{aligned} \langle \Omega | \hat{N}(t, p') \hat{O}(\tau, p' - p) \hat{N}(0, p) | \Omega \rangle = \\ \sum_{i,j} \langle \Omega | \hat{N}(p') | N_j \rangle e^{-\int dt H} \langle N_j | \hat{O}(\tau, p' - p) | N_i \rangle e^{-\int dt H} \langle N_i | \hat{N}(p) | \Omega \rangle = \\ \sum_{i,j} \langle \Omega | \hat{N}(p') | N_j \rangle e^{-E_j(t-\tau)} \underbrace{\langle N_j | \hat{O}(\tau, p' - p) | N_i \rangle}_{\text{Operator Matrix Element}} e^{-E_i\tau} \langle N_i | \hat{N}(p) | \Omega \rangle \end{aligned}$$

Electric & Magnetic form factors

Matrix Elements of $V_\mu \rightarrow$ Dirac (F_1) and Pauli (F_2) form factors

$$\langle N(p_f) | V^\mu(q) | N(p_i) \rangle = \bar{u}(p_f) \left[\gamma^\mu F_1(q^2) + \sigma^{\mu\nu} q_\nu \frac{F_2(q^2)}{2M} \right] u(p_i)$$

Define Sachs Electric (G_E) and Magnetic (G_M) form factors

$$G_E(q^2) = F_1(q^2) - \frac{q^2}{4M^2} F_2(q^2), \quad G_M(q^2) = F_1(q^2) + F_2(q^2)$$

Challenges to obtaining high precision results for matrix elements within nucleon states

- **High Statistics: $O(1,000,000)$ measurements**
- **Demonstrating control over all Systematic Errors:**
 - Excited States Contamination (ESC)
 - Q^2 behavior of form factors
 - Non-perturbative renormalization of bilinear operators (RI_{smom} scheme)
 - Finite volume effects
 - Chiral extrapolation to physical m_u and m_d (simulate at physical point)
 - Extrapolation to the continuum limit (lattice spacing $a \rightarrow 0$)

Perform simulations on ensembles with multiple values of

- Lattice size: $M_\pi L \rightarrow \infty$
- Light quark masses: \rightarrow physical m_u and m_d
- Lattice spacing: $a \rightarrow 0$

Analyzing lattice data $\Omega(a, M_\pi, M_\pi L)$: Simultaneous CCFV fits versus $a, M_\pi^2, M_\pi L$

Include leading order corrections to fit lattice data w.r.t.

- Lattice spacing: a
- Dependence on light quark mass: $m_q \sim M_\pi^2$
- Finite volume: $M_\pi L$

$$r_A^2(a, M_\pi, M_\pi L) = c_0 + c_1 a + c_2 M_\pi^2 + c_3 M_\pi^2 e^{-M_\pi L} + \dots$$

Toolkit

- Multigrid Dirac inverter \rightarrow propagator $S_F = D^{-1}\eta$
- Truncated solver method with bias correction (AMA)
- Coherent source sequential propagator
- Deflation + hierarchical probing
- High Statistics
- 3-5 values of t_{sep} with smeared sources for S_F
- 2-, 3-, n-state fits to multiple values of t_{sep}
- Non-perturbative methods for renormalization constants
- Combined extrapolation in a , M_π , $M_\pi L$ (CCFV)
- Variation of results with CCFV extrapolation Ansatz

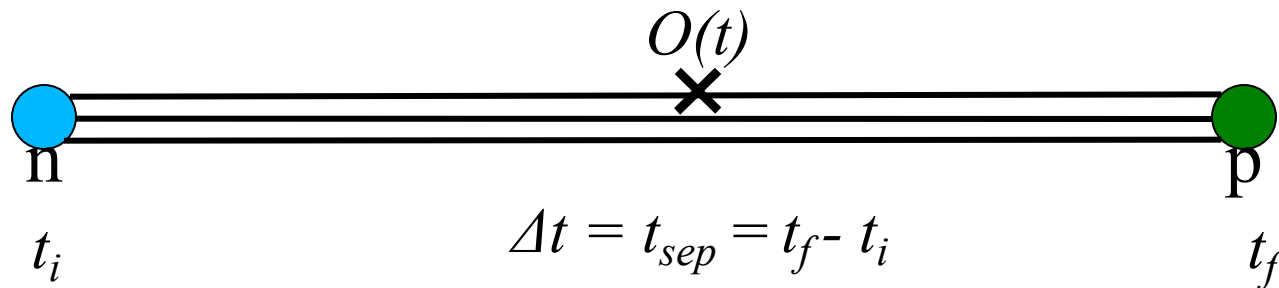
Controlling excited-state contamination: n-state fit

$$\Gamma^2(t) = |A_0|^2 e^{-M_0 t} + |A_1|^2 e^{-M_1 t} + |A_2|^2 e^{-M_2 t} + |A_3|^2 e^{-M_3 t} + \dots$$

$$\Gamma^3(t, \Delta t) = |A_0|^2 \langle 0 | O | 0 \rangle e^{-M_0 \Delta t} + |A_1|^2 \langle 1 | O | 1 \rangle e^{-M_1 \Delta t} + \\ A_0 A_1^* \langle 0 | O | 1 \rangle e^{-M_0 \Delta t} e^{-\Delta M (\Delta t - t)} + A_0^* A_1 \langle 1 | O | 0 \rangle e^{-\Delta M t} e^{-M_0 \Delta t} + \dots$$

M_0, M_1, \dots masses of the ground & excited states

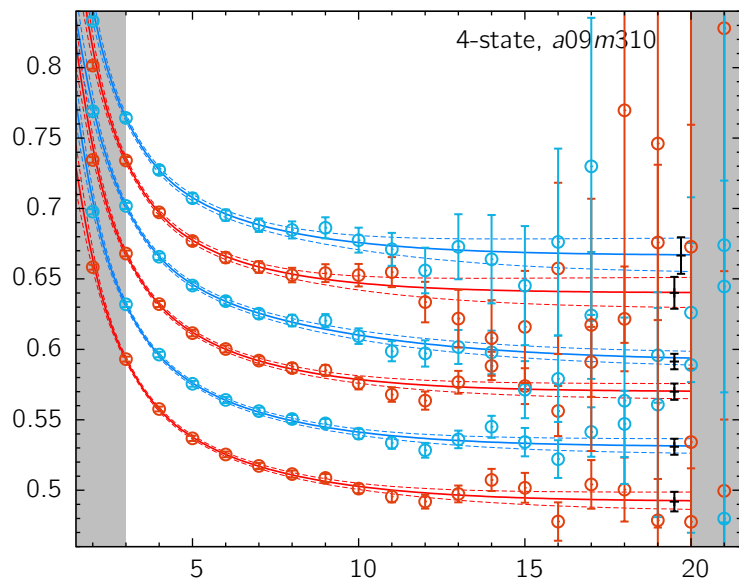
A_0, A_1, \dots corresponding amplitudes



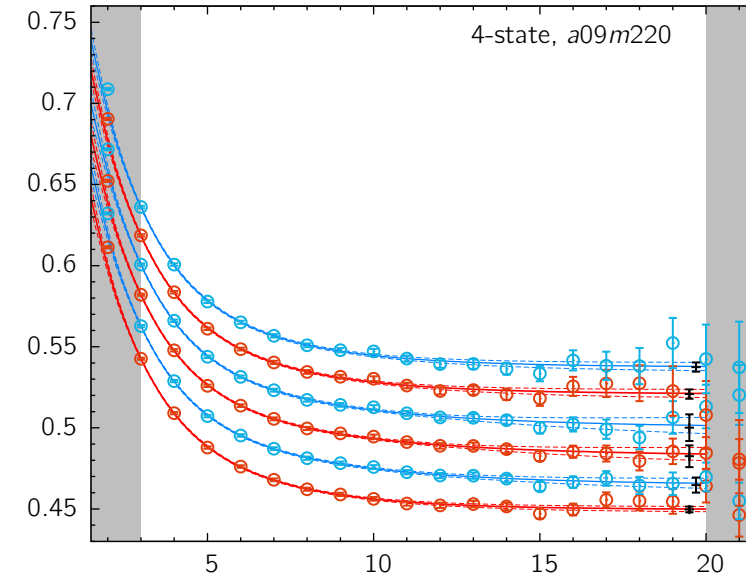
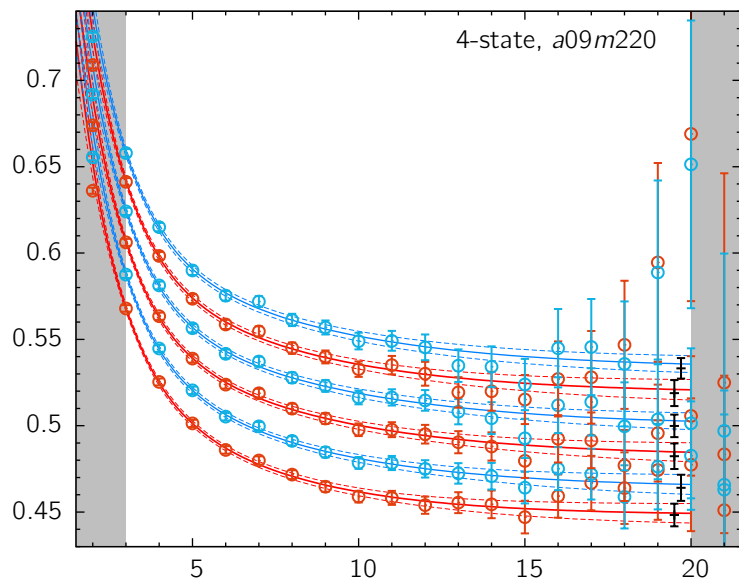
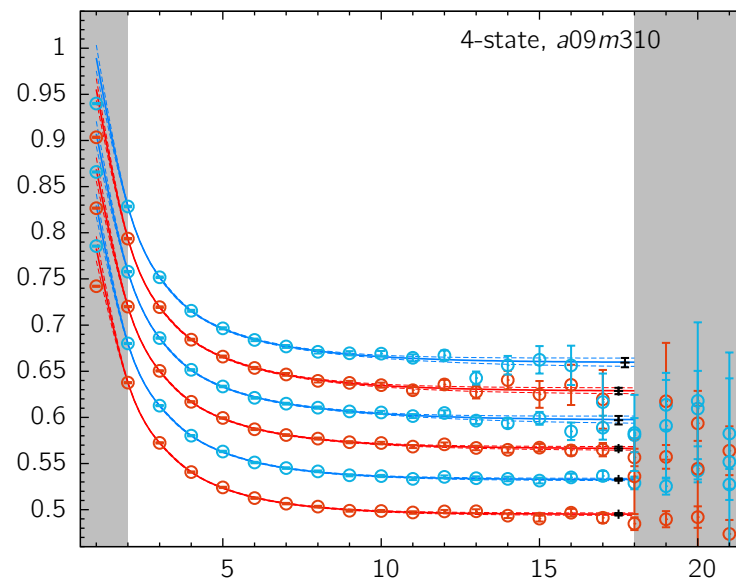
Make a simultaneous fit to data at multiple $\Delta t = t_{sep} = t_f - t_i$

KEY quantity to control: M_1 (first excited state mass)

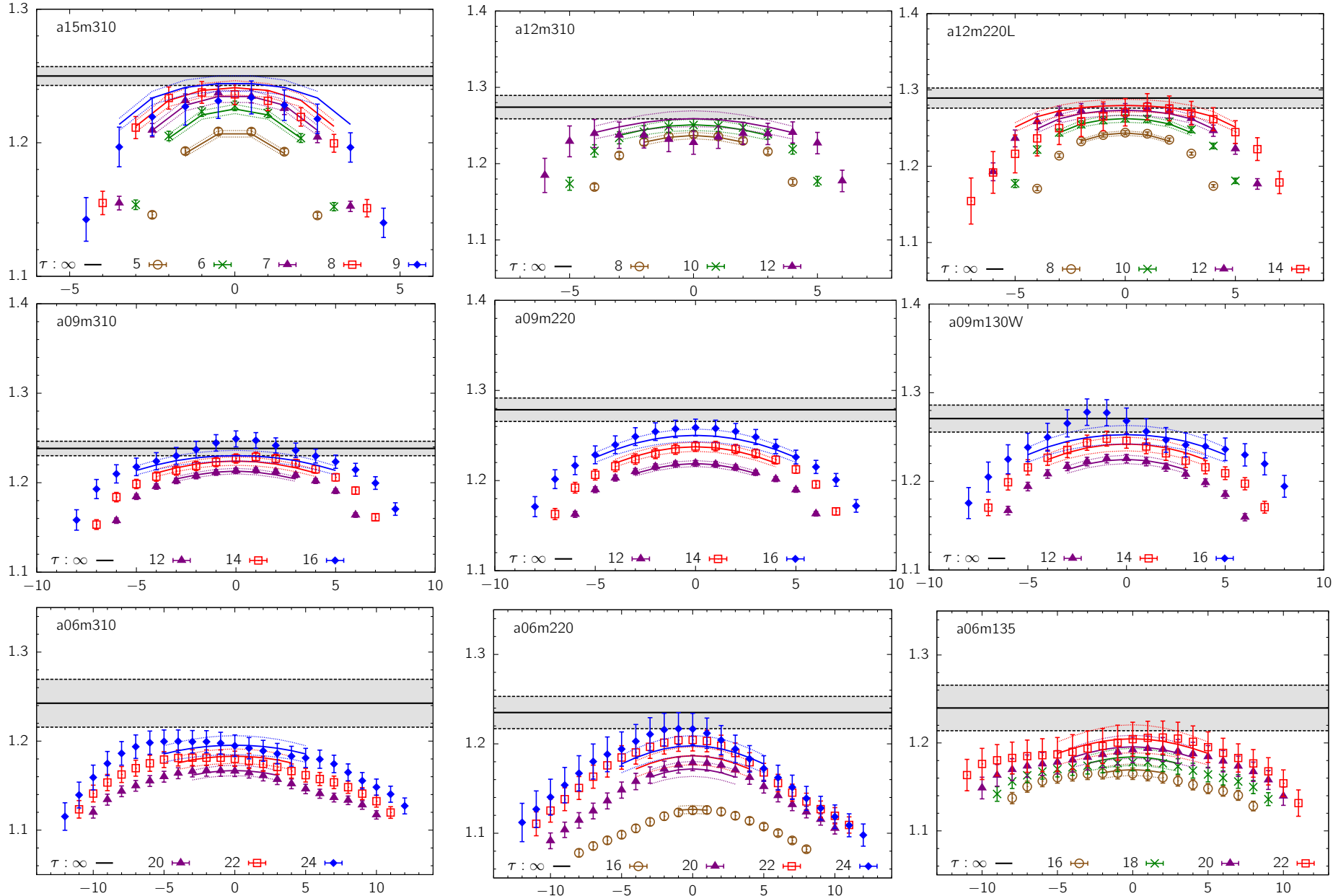
4-state fit to 2-point correlation function



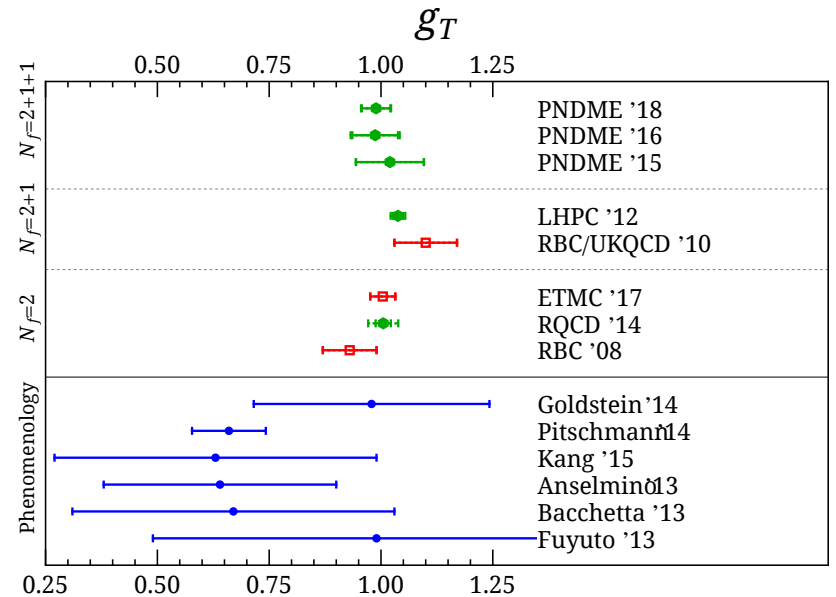
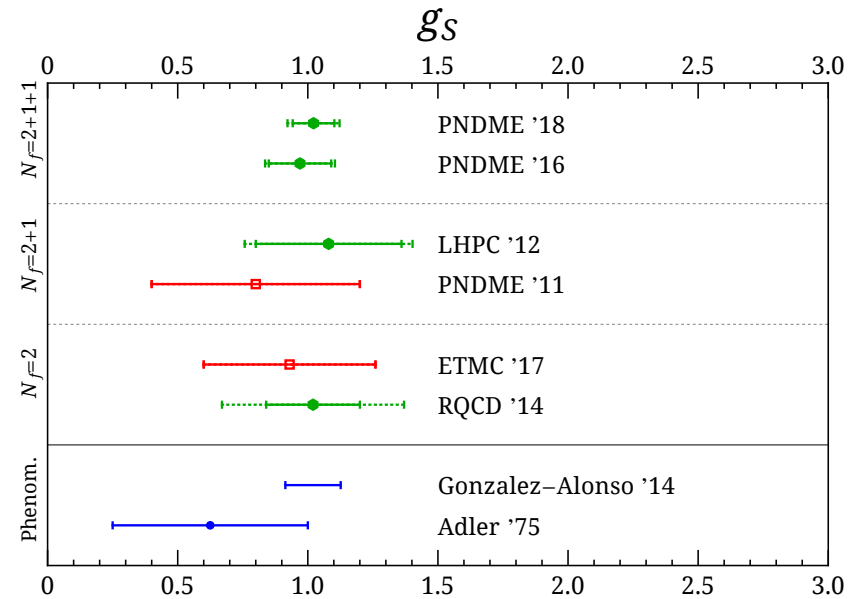
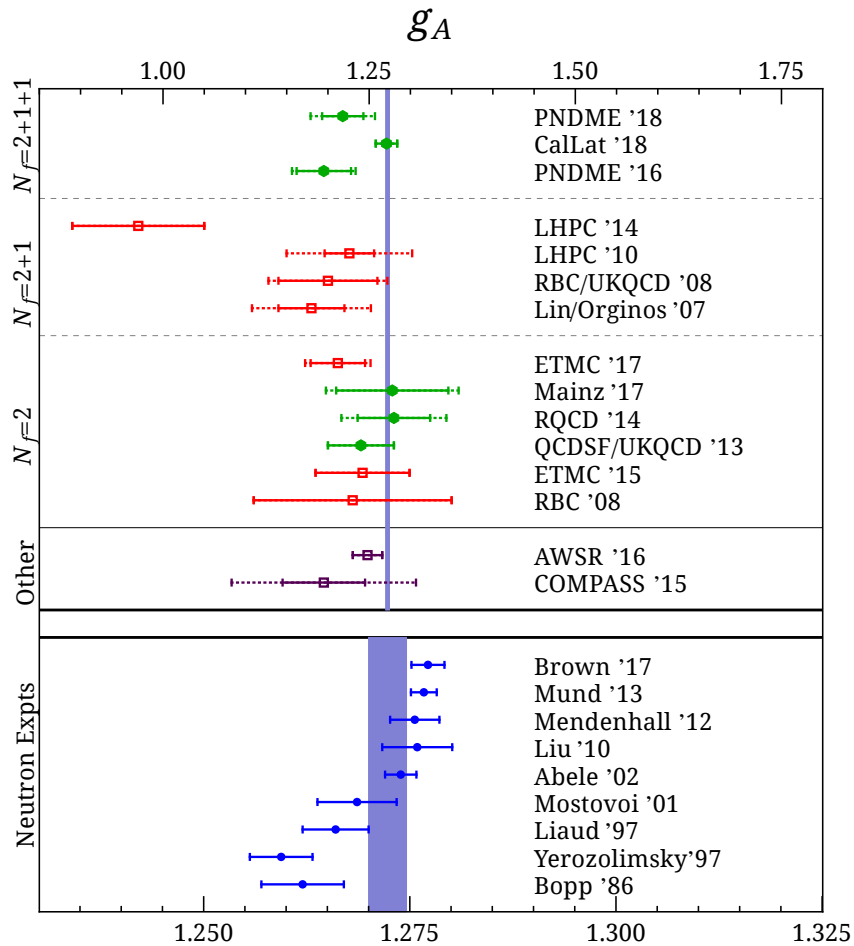
4X



g_A : Excited State Contamination



Status 2018: Isovector g_A , g_S , g_T



g_A^{u-d} : PNDME & CalLat agree within errors on 7 ensembles

CalLat: Nature: <https://doi.org/10.1038/s41586-018-0161-8>

PNDME: Gupta et al, Phys. Rev. D98 (2018) 034503

	PNDME	CalLat
a15m310	1.228(25)	1.215(12)
a12m310	1.251(19)	1.214(13)
a12m220S	1.224(44)	1.272(28)
a12m220	1.234(25)	1.259(15)
a12m220L	1.262(17)	1.252(21)
a09m310	1.235(15)	1.236(11)
a09m220	1.260(19)	1.253(09)

CalLat uses a variant of the summation method

Difference comes from the Chiral-Continuum fits:

- CalLat chiral fit anchored by heavier pion masses
- CalLat have not yet analyzed the $a=0.06\text{fm}$ lattices

Steps in the FF calculations

- Calculate matrix elements for different t_{sep}
- Control excited-state contamination: $p=0$, $p \neq 0$
- From different Lorentz components of the currents extract various form factors $G_i(q^2)$
- Fit Q^2 behavior of $G_i(q^2)$: (dipole, z-expansion, ...)
- Calculate $r_i(a, M_\pi, M_\pi L)$: $\langle r_i^2 \rangle = -\frac{6}{dq^2} \left[\frac{\hat{G}_i(q^2)}{\hat{G}_i(0)} \right]_{q^2=0}$
- Extrapolate r_i ($a \rightarrow 0$, $M_\pi L \rightarrow \infty$, $M_\pi \rightarrow 135 \text{ MeV}$)

Electric & Magnetic form factors

Matrix Elements of $V_\mu \rightarrow$ Dirac (F_1) and Pauli (F_2) form factors

$$\langle N(p_f) | V^\mu(q) | N(p_i) \rangle = \bar{u}(p_f) \left[\gamma^\mu F_1(q^2) + \sigma^{\mu\nu} q_\nu \frac{F_2(q^2)}{2M} \right] u(p_i)$$

Define Sachs Electric (G_E) and Magnetic (G_M) form factors

$$G_E(q^2) = F_1(q^2) - \frac{q^2}{4M^2} F_2(q^2), \quad G_M(q^2) = F_1(q^2) + F_2(q^2)$$

Extracting EM form factors

$$\sqrt{2E_p(M_N + E_p)} \operatorname{Re}(R_i) = -\epsilon_{ij3} q_j G_M$$

$$\sqrt{2E_p(M_N + E_p)} \operatorname{Im}(R_i) = q_i G_E$$

$$\sqrt{2E_p(M_N + E_p)} \operatorname{Re}(R_4) = (M_N + E_p) G_E$$

Each matrix element gives one form factor

ESC in $\operatorname{Im}(R_i)$ is large

Experimental Results

$$r_E = 0.875(6) \text{ fm}$$

Electron scattering

$$r_E = 0.8409(4) \text{ fm}$$

Muonic hydrogen

$$r_M = 0.86(3) \text{ fm}$$

$$\mu_P = 2.7928$$

$$\mu_N = -1.9130$$

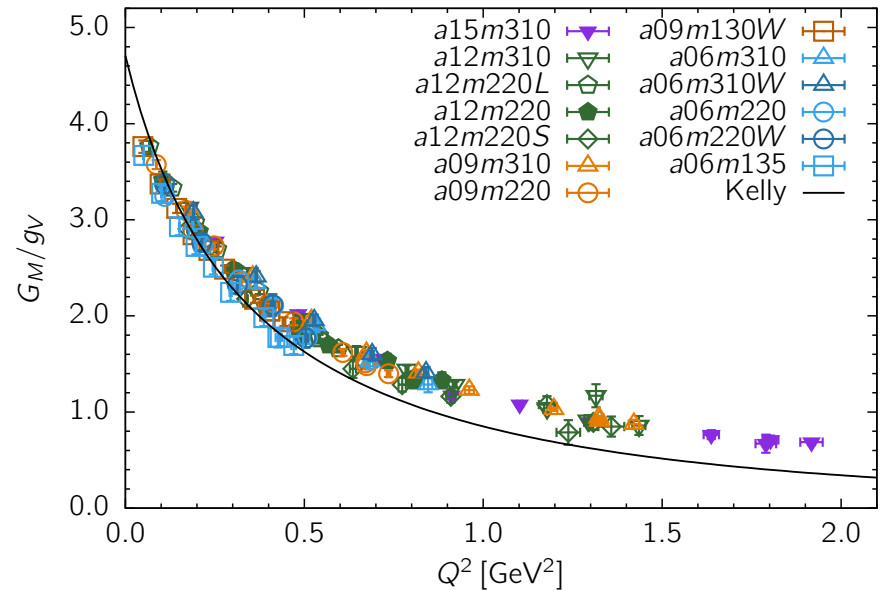
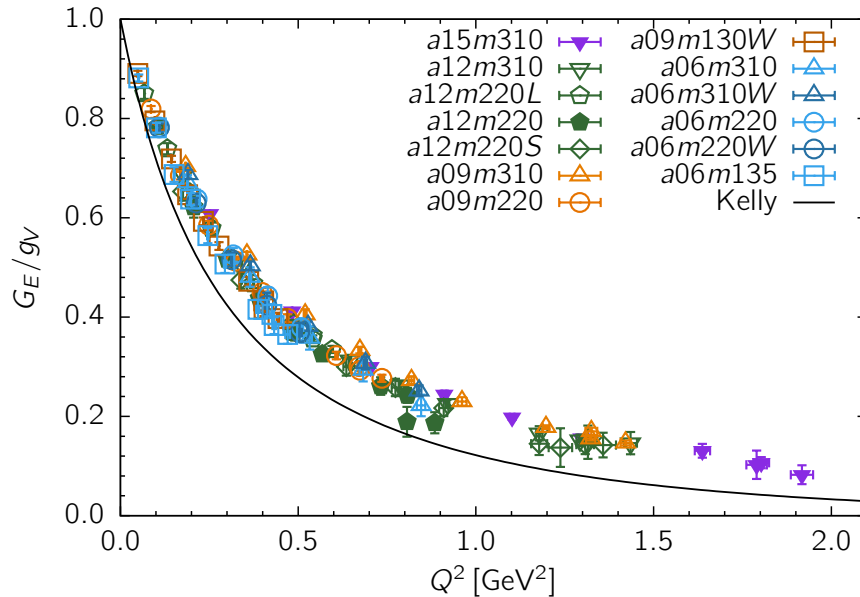
$$r_E^{p-n} = 0.93 \text{ fm}$$

$$r_M^{p-n} = 0.87 \text{ fm}$$

Isovector radii

We will focus on the primary quantities $G_E(Q^2)$, $G_M(Q^2)$

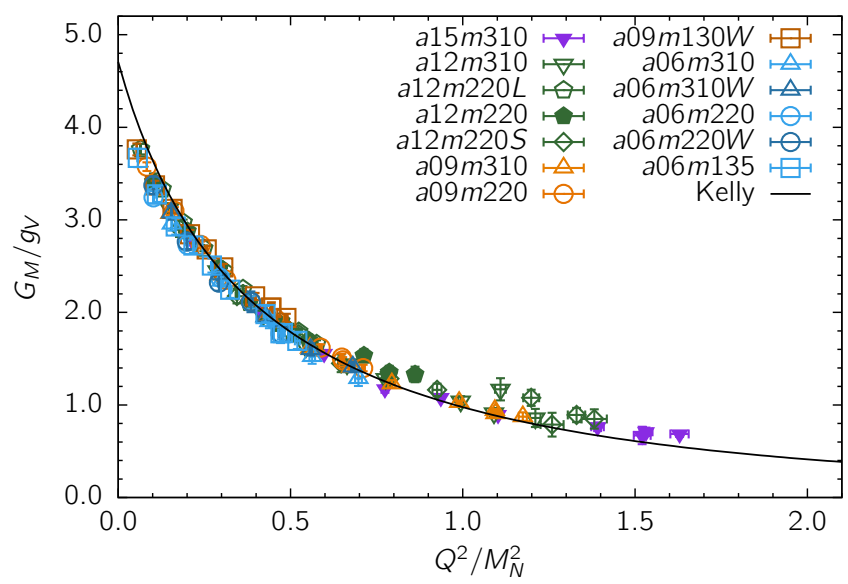
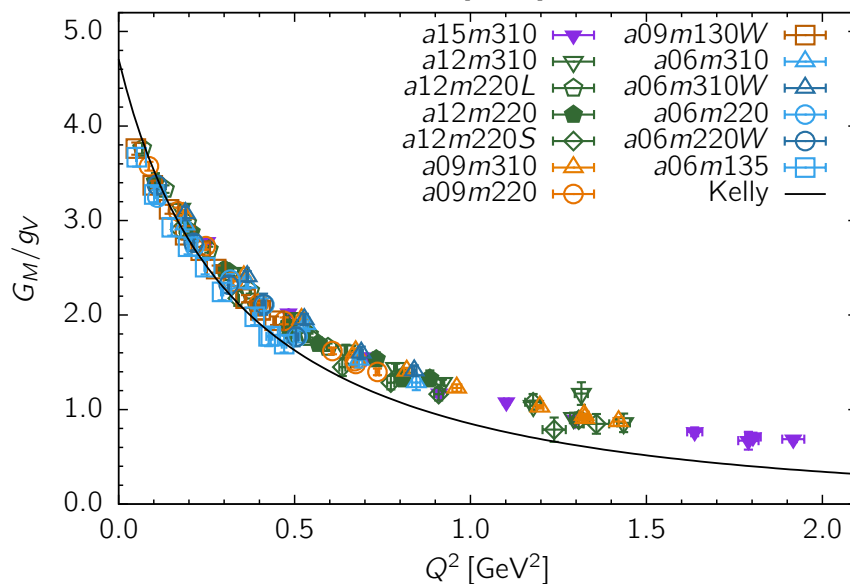
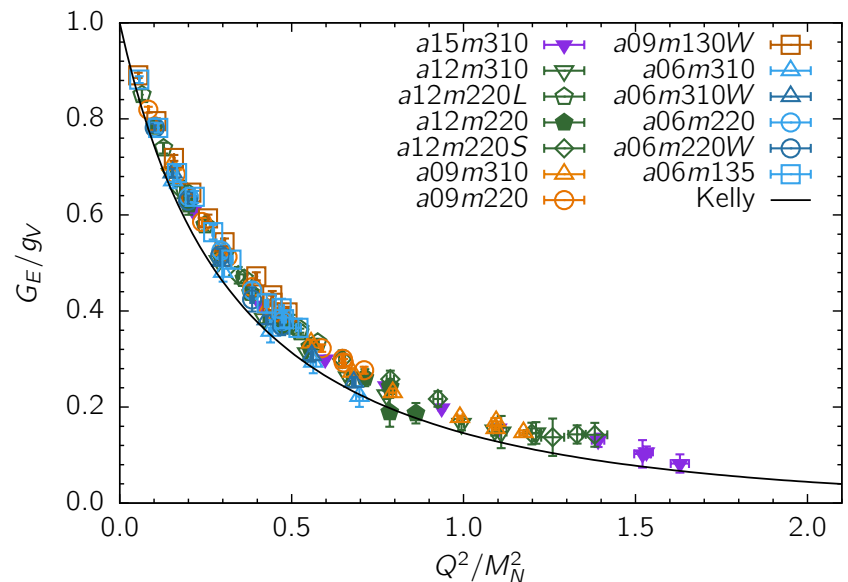
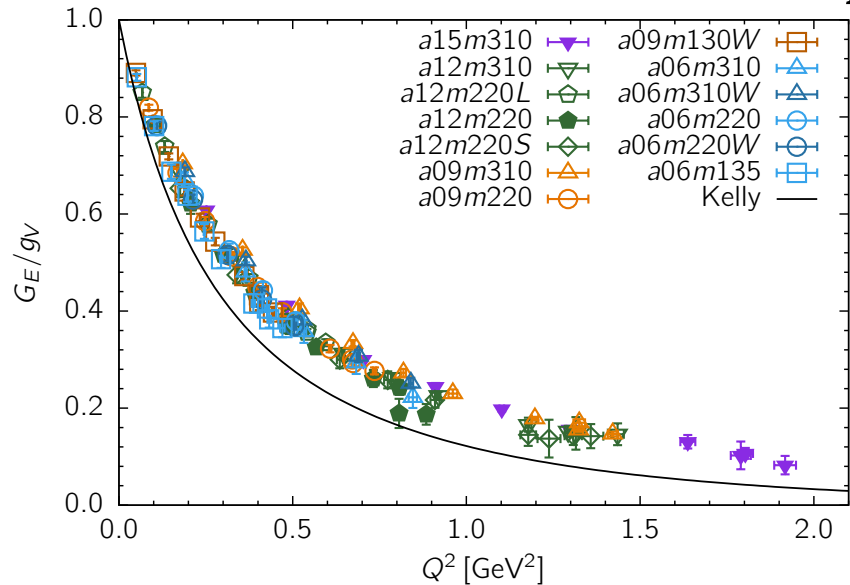
Clover-on-HISQ data



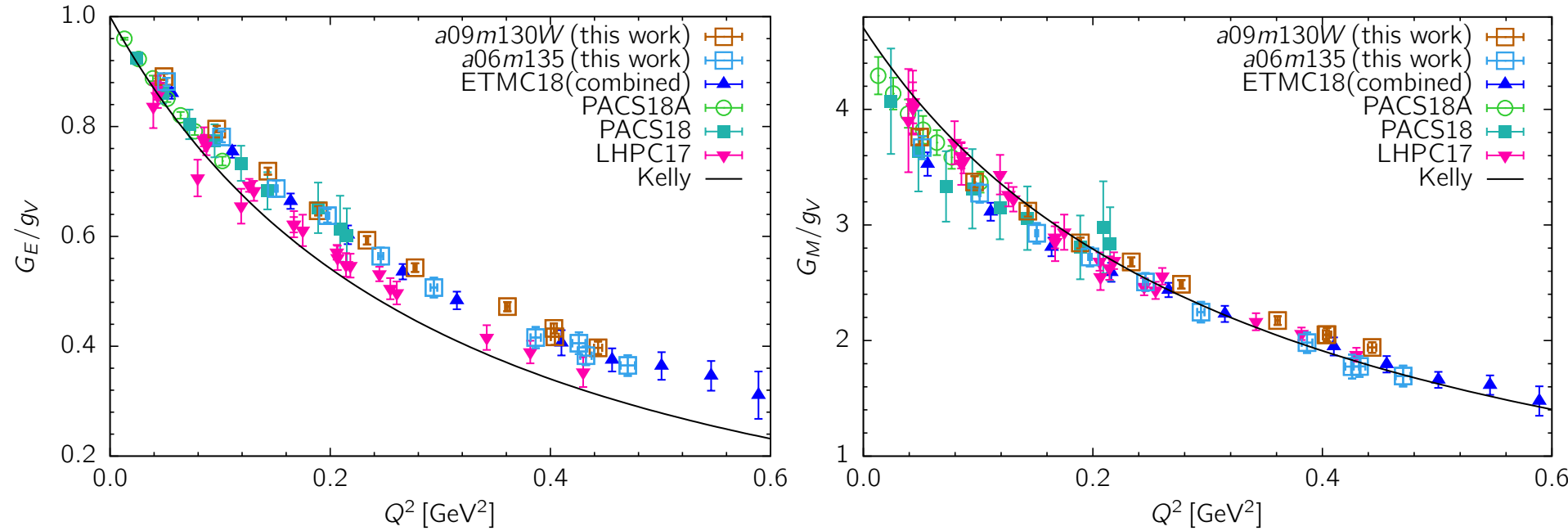
Does collapse of data into a single curve imply that $G_E(Q^2)$, $G_M(Q^2)$ are insensitive to the lattice spacing, pion mass, lattice volume?

The phenomenological Kelly curve shown for reference.
It is not the target of lattice calculations!

Fits vs. Q^2 or $\frac{Q^2}{M_N^2}$: Clover-on-HISQ data

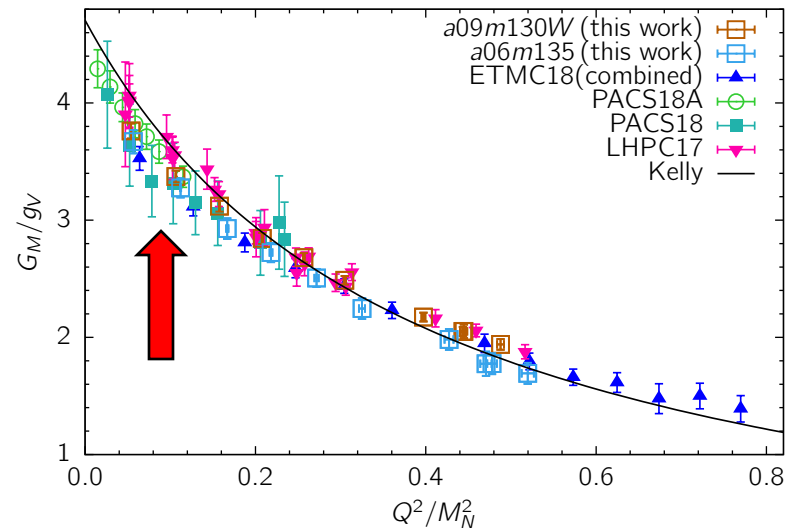
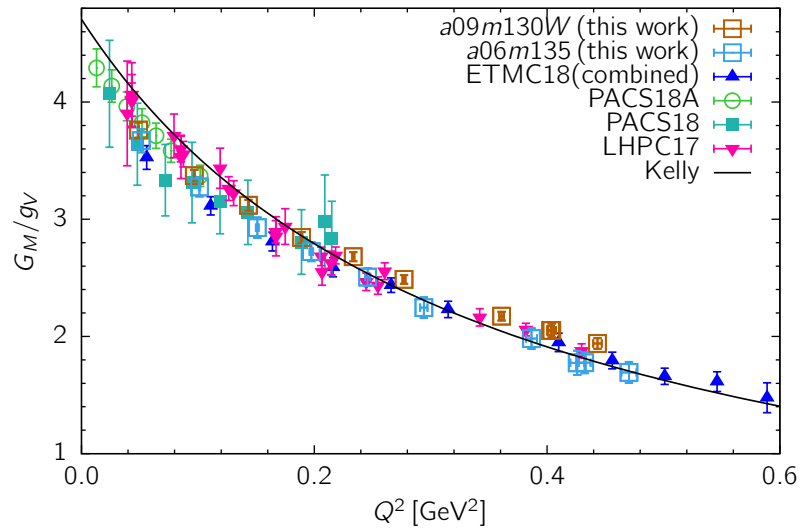
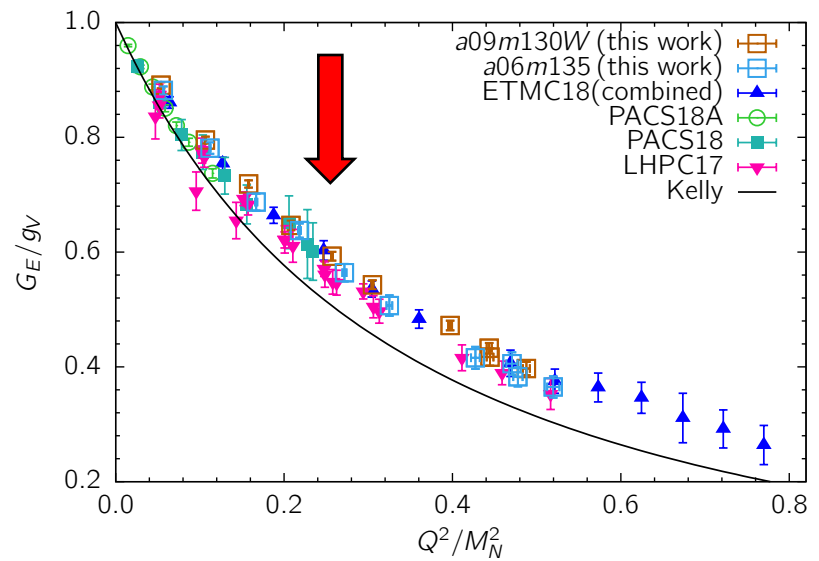
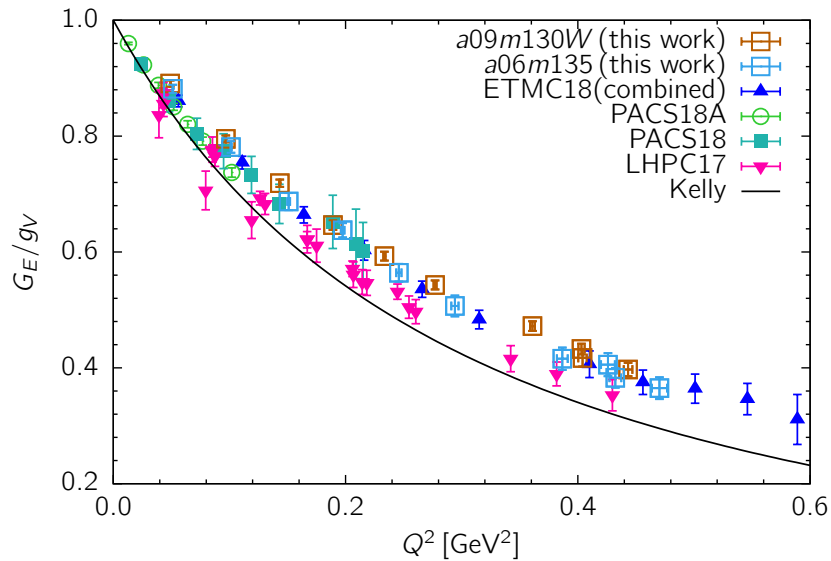


Comparison of world $M_\pi \sim 135\text{MeV}$ data



$M_\pi \sim 135\text{MeV}$ data for $G_E(Q^2)$, $G_M(Q^2)$ from different collaborations also collapse close to a single curve.

Comparison of $M_\pi \sim 135\text{MeV}$ data



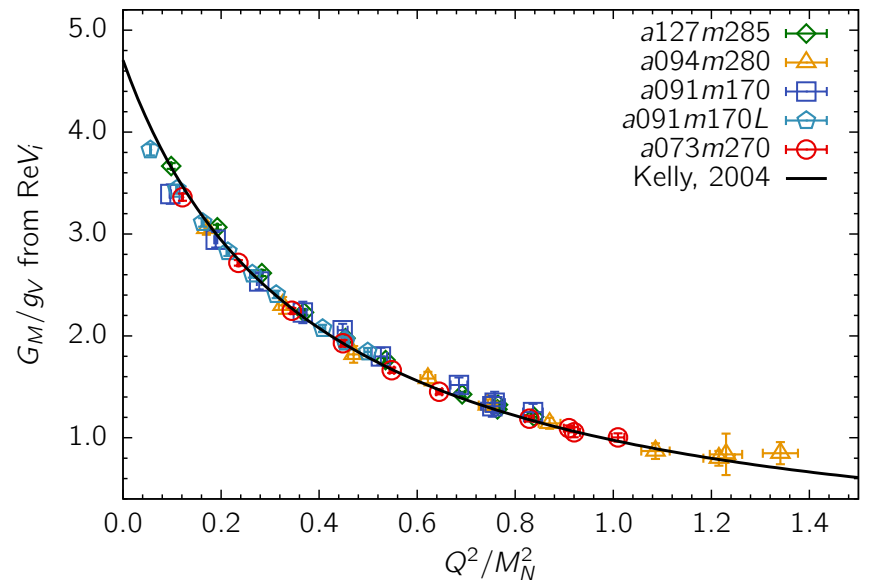
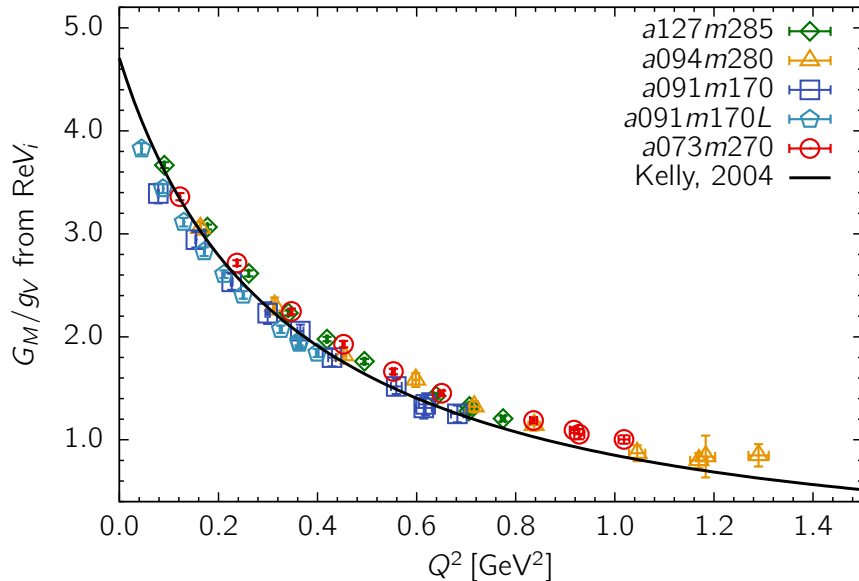
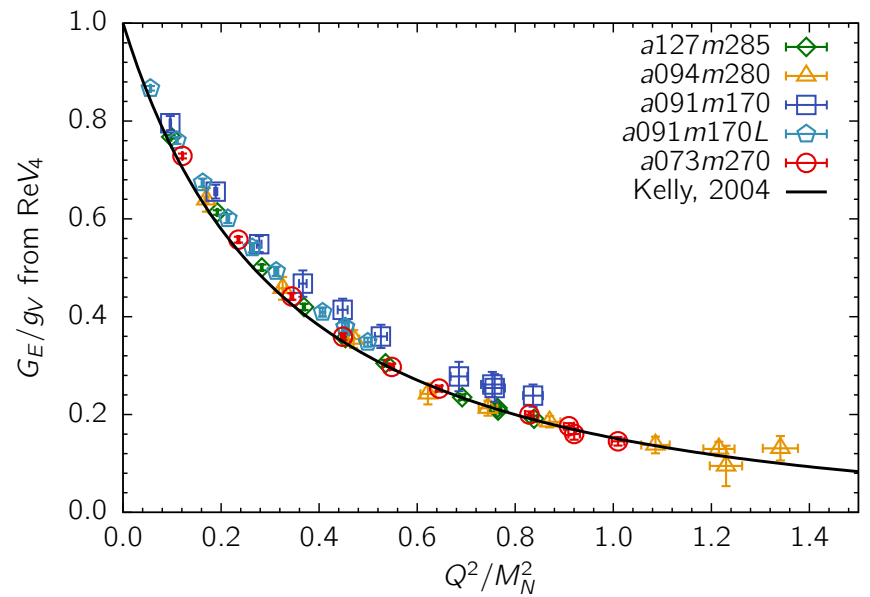
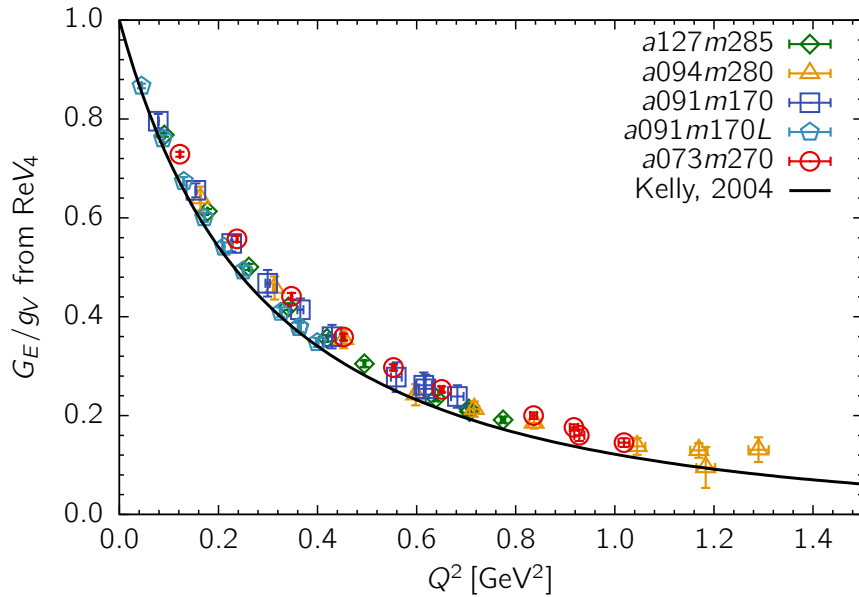
Collapse into a single curve more evident vs. $\frac{Q^2}{M_N^2}$

Does collapse versus Q^2/M_N^2 imply that $G_E(Q^2)$, $G_M(Q^2)$ are insensitive to

- the lattice spacing,
- pion mass,
- lattice volume,
- number of flavors: 2, 2+1, 2+1+1?

Clover-on-clover data

NME unpublished: 5 ensembles with ~ 2000 configs each



Kelly Parameterization

Kelly parameterization of the experimental data for G_E , G_M

$$\hat{G}_X(Q^2) = \frac{\hat{G}(0) \sum_{k=0}^n a_k \tau^k}{\left\{ 1 + \sum_{k=1}^{n+2} b_k \tau^k \right\}}, \quad \hat{G}_Y(Q^2) = \frac{A\tau}{1 + B\tau} \frac{1}{\left(1 + Q^2/0.71\text{GeV}^2\right)^2}$$

where $\tau = Q^2/4\mathcal{M}^2$. The parameters \mathcal{M} , $G(0)$, a_k , b_k , A , and B are determined from fit to the data.

Do the "experimental data" that are fit using the Kelly parameterization have all significant corrections included?

z-expansion

The form factors are analytic functions of Q^2 below a cut starting at n-particle threshold t_{cut} .

A model independent approach is the z -expansion:

$$\hat{G}(Q^2) = \sum_{k=0}^{\infty} a_k z (Q^2)^k \quad \text{with} \quad z = \frac{\sqrt{t_{cut} + Q^2} - \sqrt{t_{cut} + Q_0^2}}{\sqrt{t_{cut} + Q^2} + \sqrt{t_{cut} + Q_0^2}}$$

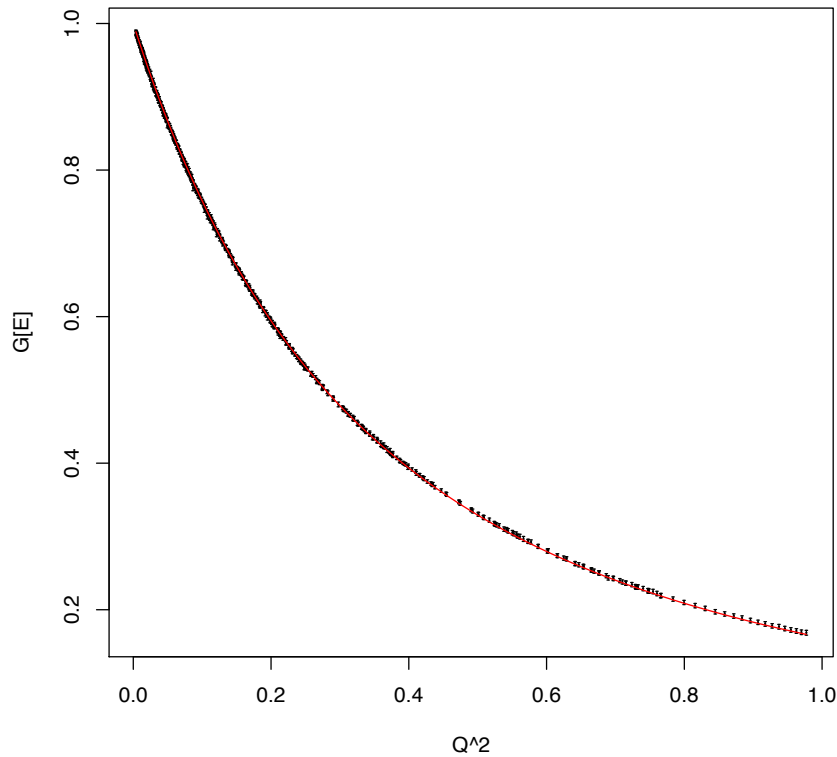
with $t_{cut} = 4m_\pi^2$ for $G_{E,M}$ and $t_{cut} = 9m_\pi^2$ for G_A . We choose $Q_0 = 0$

Incorporate $1/Q^4$ behavior as $Q^2 \rightarrow \infty$ via sum rules

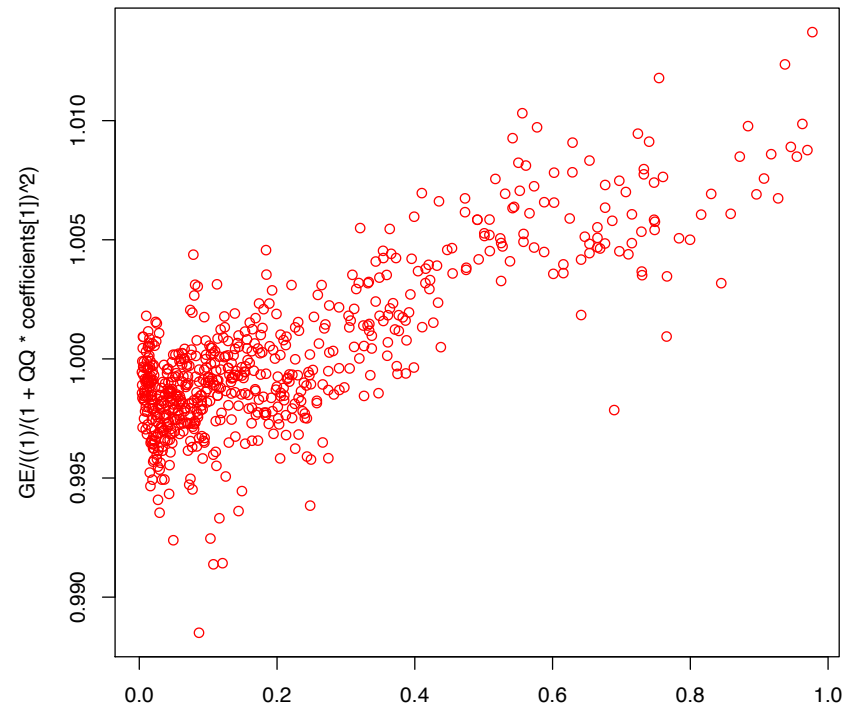
Impose Bound $|a_k| < 5$

Results independent of truncation for $k \geq 4$

Is dipole a good model?



dipole fit to Mainz data for G_E



Mainz G_E data
dipole fit

Yes for G_E ($\sim 1\%$), not so for G_M ($\sim 6\%$)

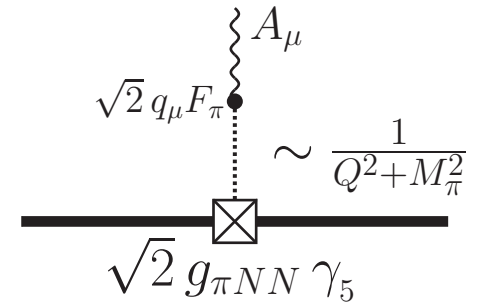
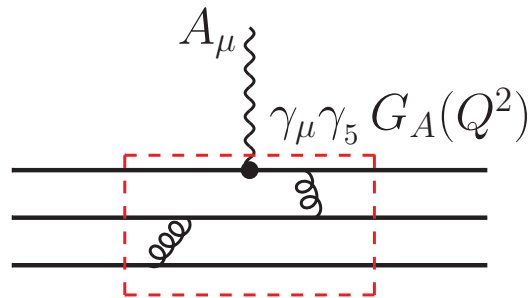
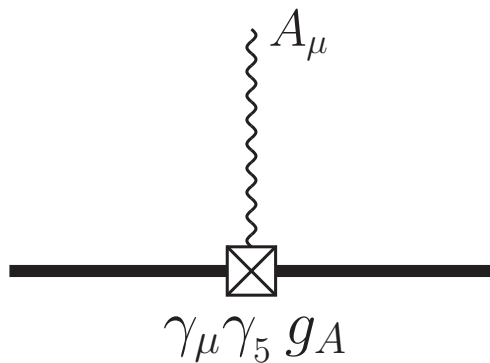
Thanks to D. Higinbotham for providing his version of the binned Mainz data

Summary:

Electric and Magnetic form factors

- $G_E(Q^2), G_M(Q^2)$ show small variation with $a, M_\pi, M_\pi L, N_f$: PNDME (11 clover-on-HISQ ensembles) and NME data (5 clover-on-clover ensembles) collapse onto a single curve
- The curve becomes narrower and closer to the “Kelly curve” when plotted versus Q^2/M_N^2 as compared to Q^2
- World data for $G_E(Q^2), G_M(Q^2)$ with $M_\pi \sim 135\text{MeV}$ also collapse to this curve
- Deviations from the “Kelly curve” are within possible errors
 - Excited-state effects are large at small Q^2 for $G_M(Q^2)$
 - Excited-state effects in G_E are small for $Q^2 \sim 0$, but increase with Q^2
 - Lattice artifacts increase as Q^2 increases

Axial-vector form factors



On the lattice we can calculate 3 form factors from ME of V_μ and A_μ :

- Axial: G_A
- Induced pseudoscalar: \tilde{G}_P
- Pseudoscalar: G_P

$$\langle N(p_f) | A^\mu(q) | N(p_i) \rangle = \bar{u}(p_f) \left[\gamma^\mu G_A(q^2) + q_\mu \frac{\tilde{G}_P(q^2)}{2M} \right] \gamma_5 u(p_i)$$

$$\langle N(p_f) | P(q) | N(p_i) \rangle = \bar{u}(p_f) G_P(q^2) \gamma_5 u(p_i)$$

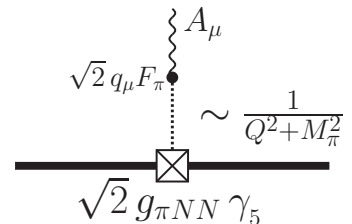
The 3 form factors are related by PCAC $\partial_\mu A_\mu = 2mP$

PCAC ($\partial_\mu A_\mu = 2\hat{m}P$) requires

$$2\hat{m}G_P(Q^2) = 2M_N G_A(Q^2) - \frac{Q^2}{2M_N} \tilde{G}_P(Q^2)$$

Pion pole-dominance hypothesis

$$\tilde{G}_P(Q^2) = G_A(Q^2) \left[\frac{4M_N^2}{Q^2 + M_\pi^2} \right]$$



If pion pole-dominance holds

\Rightarrow there is only one independent form factor

Goldberger-Treiman relation

$$F_\pi g_{\pi NN} = M_N g_A$$

Dipole ansatz for Q^2 behavior of G_A

$$G_i(q^2) = \frac{G_i(0)}{\left(1 + \frac{q^2}{M_i^2}\right)^2} \quad M_i \text{ is the dipole mass}$$

- Corresponds to exponential decaying distribution
- Has the desired $1/q^4$ behavior for $q^2 \rightarrow \infty$

The charge radii are defined as

$$\langle r_i^2 \rangle = -\frac{6}{dq^2} \left[\frac{\hat{G}_i(q^2)}{\hat{G}_i(0)} \right]_{q^2=0}$$
$$\langle r_i^2 \rangle = \frac{12}{M_i^2}$$

Experimental Results

$$r_A = 0.80(17) \text{ fm}$$

ν scattering

$$r_A = 0.74(12) \text{ fm}$$

Electroproduction

$$r_A = 0.68(16) \text{ fm}$$

Deuterium target

Extracting Axial form factors

$$\text{Im}(R_{51}) = 4 M_N \left(-\frac{q_1 q_3}{2M_N} \widetilde{G}_P \right)$$

$$\text{Im}(R_{52}) = 4 M_N \left(-\frac{q_1 q_3}{2M_N} \widetilde{G}_P \right)$$

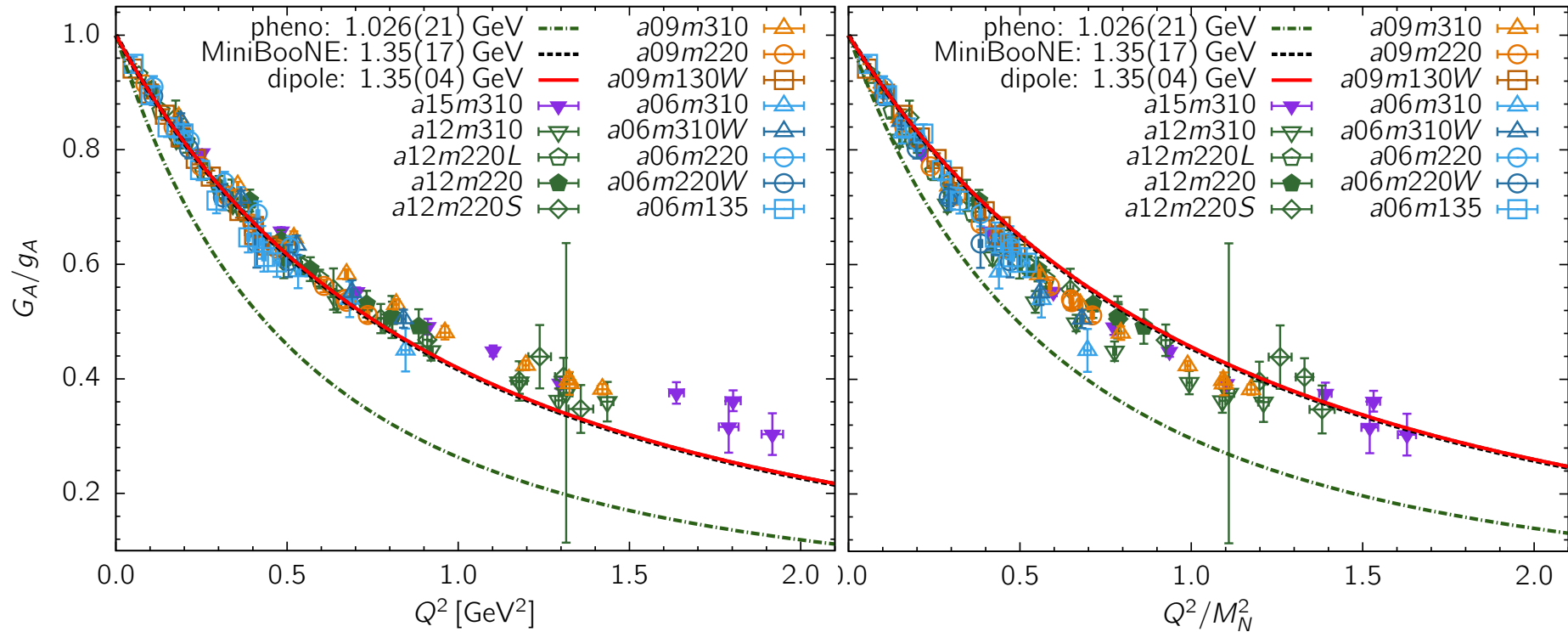
$$\text{Im}(R_{53}) = 4 M_N \left((M_N + E)G_A - \frac{q_3^2}{2M_N} \widetilde{G}_P \right)$$

$$\text{Re}(R_{54}) = 4 M_N q_3 \left(G_A + \frac{M_N - E}{2M_N} \widetilde{G}_P \right)$$

ESC in R_{54} is large

Clover-on-HISQ data

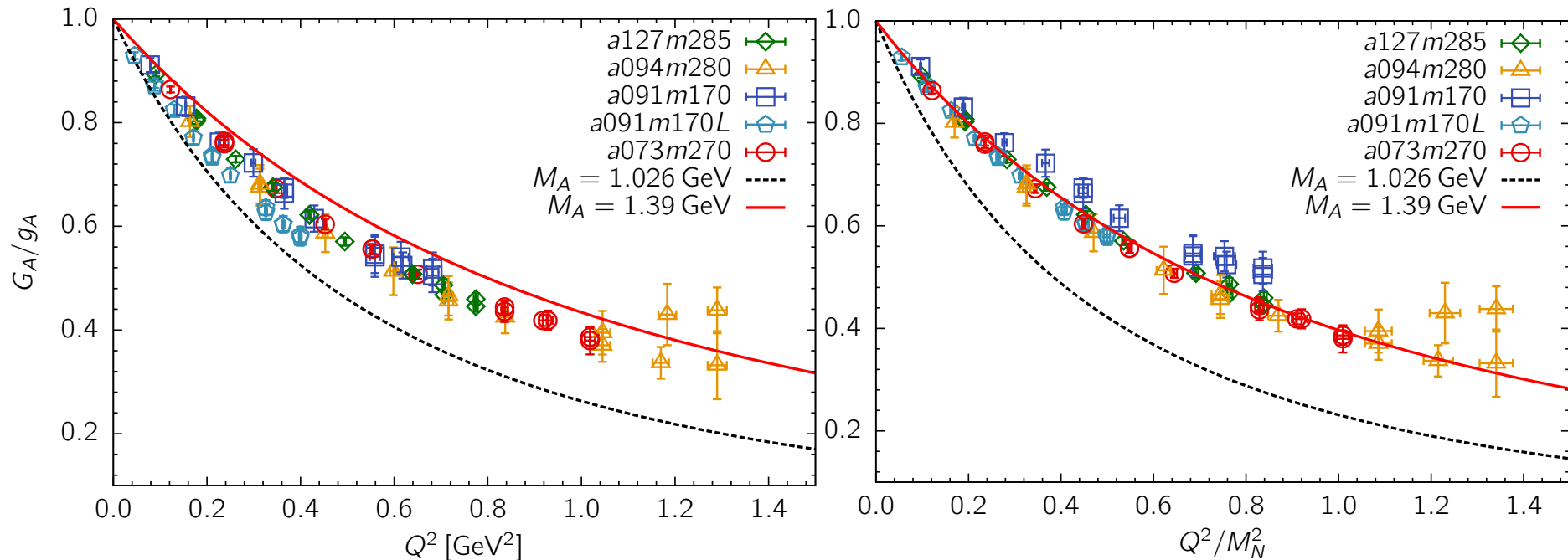
PNDME unpublished



NOTE: The two dipole curves with $M_A = 1.35$ and $M_A = 1.026$ are drawn only as a reference to quantify spread and uncertainty in the lattice data

Clover-on-clover data

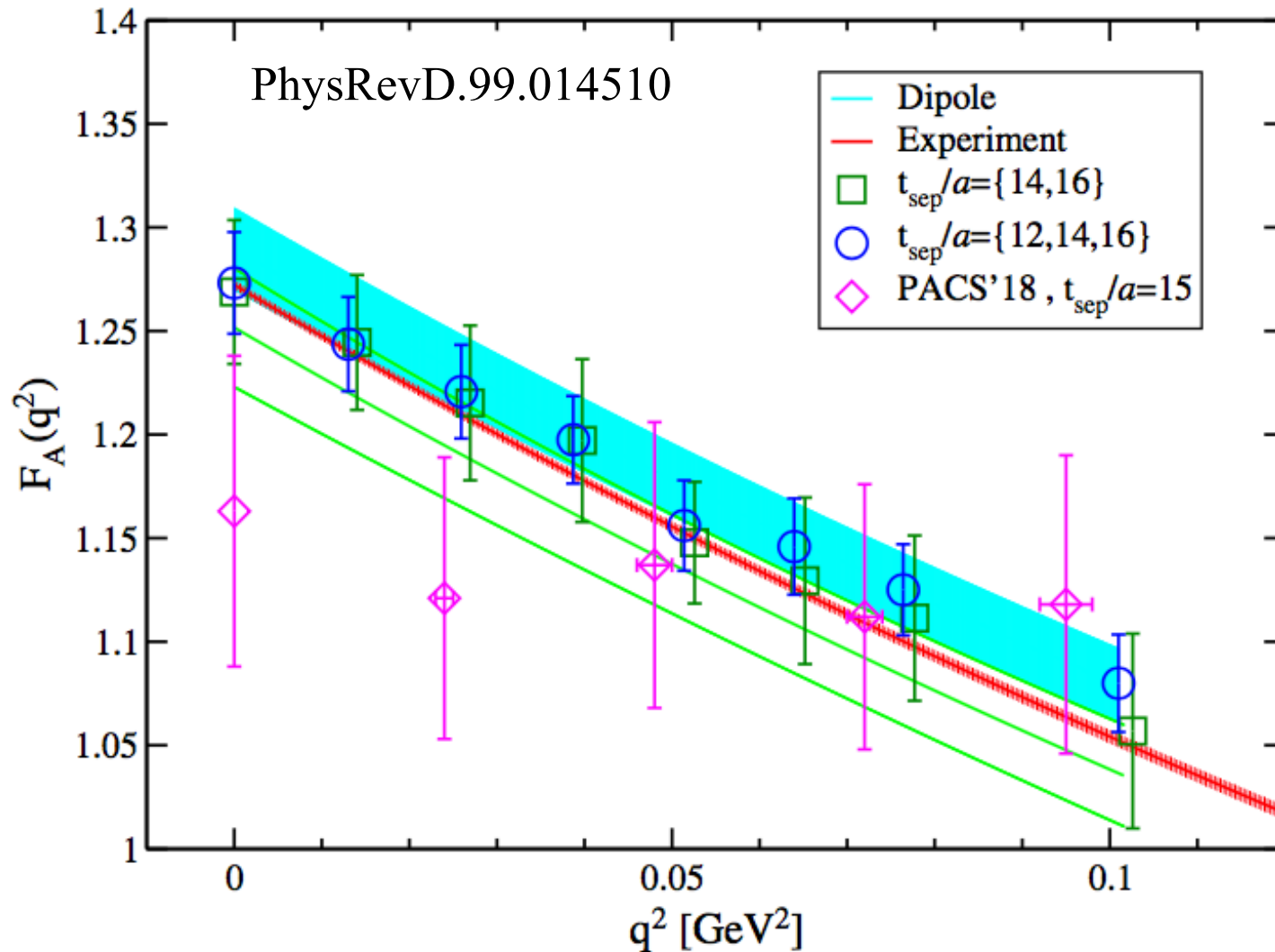
NME unpublished: 5 ensembles with ~ 2000 configs each



The lines with $M_A = 1.026$ and 1.35 GeV are drawn only as a reference

The $a091m170$ statistics (blue squares) $\rightarrow 2X$

PACS data at small Q^2



Red line (“experiment”): dipole fit with $M_A = 1.02 \text{ GeV}$

Do G_A , \widetilde{G}_p , G_p satisfy PCAC?

Brief statement of an unsolved issue

The operator relation ($\partial_\mu A_\mu = 2\hat{m}P$) holds when inserted in correlation functions in lattice data.

PCAC also implies a relation between form factors

$$2\hat{m}G_P(Q^2) = 2M_N G_A(Q^2) - \frac{Q^2}{2M_N} \tilde{G}_P(Q^2)$$

This is violated.

We have tracked the problem to ME of

$$\partial_4 A_4 \neq (E - m)A_4$$

Since this relation should hold in the ground state, what do large violations at $t_{sep} \sim 1.5$ fm imply for control over ESC?

Summary

- Data for isovector charges and form factors becoming precise at the few percent level for $Q^2 < 1 \text{ GeV}^2$
- Need to understand why the 3 form factors $G_A, \widetilde{G}_p, G_p$ do not satisfy PCAC
- Lattice values of the charge radii r_A are smaller than “phenomenological” estimates.
- Are all the systematics under control?
- Need data at smaller Q^2 to improve $\langle r_i^2 \rangle$ (PACS)
- Disconnected contributions reaching similar maturity